Thermochimica Acta 481 (2009) 46–51

Contents lists available at ScienceDirect

Thermochimica Acta

journal homepage: www.elsevier.com/locate/tca

# Thermal analysis of manganese(II) complexes of general formula $(Bu_4N)_2[MnBr_nCl_{4-n}]$

E. Styczeń [a], D. Wyrzykowski [a], M. Gazda [b], Z. Warnke [a,*]

[a] Faculty of Chemistry, University of Gdańsk, Sobieskiego 18, 80-952 Gdańsk, Poland
[b] Faculty of Physics and Mathematics, Technical University of Gdańsk, Narutowicza 11/12, 80-952 Gdańsk, Poland

ARTICLE INFO

*Article history:*
Received 14 August 2008
Received in revised form 1 October 2008
Accepted 6 October 2008
Available online 17 October 2008

*Keywords:*
Tetrahalogenomanganeses(II)
Thermal decomposition

ABSTRACT

Thermal decomposition of compounds consisting of tetrahalogenomanganese(II) anions, $[MnBr_nCl_{4-n}]^{2-}$ ($n$ = 0–4), and a tetrabutylammonium cation has been studied using the DSC, TG-FTIR, TG–MS and DTA techniques. The measurements were carried out in an argon and static air atmospheres over the temperature ranges 173–450 K (DSC) and 300–1073 K (TG). Solid products of the thermal decomposition were identified by FT-FIR spectroscopy as well as X-ray powder diffractometry.



## 1. Introduction

Owing to frequent occurrence of the chloride and bromide ligands in metallocomplexes, their spectroscopic characteristics, involving mostly metal–ligand frequencies, have inspired a number of research workers. Apart from earlier reports on the $[CoX_4]^{2-}$ [1], $[NiX_4]^{2-}$ [2], $[FeX_4]^{2-}$ [3] and $[MnX_4]^{2-}$ [4] (where X = $Cl^-$, $Br^-$) complexes, those with the same organic cation were for the first time prepared and spectroscopically characterized by Clark and Dunn [5]. Apart from the spectroscopic studies, considerable attention has been focused on structural analysis [6–16] and magnetic properties [17–22]. Additionally, the $(Bu_4N)_2[MX_4]$ (M = $Mn^{2+}$, $Co^{2+}$, $Ni^{2+}$, $Cd^{2+}$; X = $Cl^-$, $Br^-$) salts have been found to melt neat at 373 K to mobile, electrically conducting liquids [23–25].

However, to the best of our knowledge, there are no reports on thermal decomposition of compounds with the tetrahalogenometallate(II) anions. Just this was the reason which prompted us to embark on these studies. Our interest has been focused on thermal stability of the metal–ligand bond in the complex anion. Our studies have now been extended over the synthesis of some novel compounds with mixed-ligand anions of general formula $[MBr_nCl_{4-n}]^{2-}$ ($n$ = 1–3). The tetrahedral geometry of the anions was stabilized by cations of quaternary ammonium salts whose thermal decomposition had previously been reported [26]. Thus, facilitating correct interpretation of the thermal decomposition steps of the inorganic constituent.

This work is a continuation of our investigations into tetrahalogenometallates(II) [27,28], but this time a manganese(II) ion is the centre of co-ordination and a tetrabutylammonium ion, $Bu_4N^+$, acts as a counter-ion.

To investigate phase transformations, DSC curves have been recorded over the range 174–450 K. By inspection of the TG, DTG and DTA curves and using the FTIR, FT-FIR and MS techniques as well as the results of the X-ray powder diffractometry of polycrystalline samples, products of successive steps of the thermal decomposition of the $(Bu_4N)_2[MnBr_nCl_{4-n}]$ compounds have been identified. As previously, the measurements were run in argon and static air.

## 2. Experimental

The manganese(II) complex salts were obtained by a procedure described in the literature, by mixing together stoichiometric quantities of a manganese(II) halide with tetrabutylammonium chloride and/or bromide in ethanol [2].

### 2.1. Synthesis of $(Bu_4N)_2[MnCl_4]$

$MnCl_2$ (0.05 mol) was dissolved in a small quantity of ethanol and the solution was added to ethanolic solution of $Bu_4NCl$ (0.1 mol) (found: C, 56.8; N, 4.1; H, 10.9. Calcd. for $(Bu_4N)_2[MnCl_4]$, C, 56.3; N, 4.1; H, 10.7%).

* Corresponding author. Tel.: +48 58 5235360; fax: +48 58 3410357.
*E-mail address:* warnke@chem.univ.gda.pl (Z. Warnke).

0040-6031/$ – see front matter © 2008 Elsevier B.V. All rights reserved.
doi:10.1016/j.tca.2008.10.003

### 2.2. Synthesis of $(Bu_4N)_2[MnBr_4]$

$(Bu_4N)_2[MnBr_4]$ was also prepared as described, by using $MnBr_2$ (0.05 mol) and $Bu_4NBr$ (found: C, 44.7; N, 3.0; H, 8.7. Calcd. for $(Bu_4N)_2[MnBr_4]$, C, 44.7; N, 3.2; H, 8.5%).

### 2.3. Synthesis of $(Bu_4N)_2$ $[MnBrCl_3]$

$MnCl_2$ (0.05 mol) was dissolved in a small quantity of ethanol and the solution was added to an equimolar mixture (0.05 mol each) of $Bu_4NCl$ and $Bu_4NBr$ in ethanol (found: C, 52.9; N, 4.4; H, 10.1. Calcd. for $(Bu_4N)_2[MnBrCl_3]$, C, 52.9; N, 3.9; H, 10.0%).

### 2.4. Synthesis of $(Bu_4N)_2[MnBr_3Cl]$

$(Bu_4N)_2[MnBr_3Cl]$ was prepared as described, but $MnBr_2$ (0.05 mol) was used as a manganese halide (found: C, 47.4; N, 3.4; H, 9.1. Calcd. for $(Bu_4N)_2[MnBr_3Cl]$, C, 47.1; N, 3.4; H, 8.9%).

### 2.5. Synthesis of $(Bu_4N)_2[MnBr_2Cl_2]$

$MnCl_2$ (0.05 mol) was dissolved in a small quantity of ethanol and the solution was added to an ethanolic solution of $Bu_4NBr$ (0.01 mol) (found: C, 49.9; N, 4.2; H, 9.6. Calcd. for $(Bu_4N)_2[MnBr_2Cl_2]$, C, 49.9; N, 3.7; H, 9.4%).

### 2.6. Instrumental

The FT-FIR spectra were recorded on a BRUKER IFS 66 spectrophotometer in PE over the 650–50 $cm^{-1}$ range.

The TG-FTIR analyses in argon (Ar 5.0) were run on a Netzsch TG 209 apparatus coupled with a Bruker FTIR IFS66 spectrophotometer (range 298–1073 K, corundum crucible, sample mass *ca*. 12 mg, heating rate 15 K/min, flow rate of the carrier gas 18 mL/min).

The TG-DTA measurements in helium were carried out on SDT 2960 (TA Instruments) apparatus (range 290–1273 K, corundum crucible, sample mass *ca.* 4–5 mg, heating rate 5 K/min). The SDT apparatus was connected on-line with the quadrupole mass spectrometer QMD 300 Thermostar (Balzers).

The course of thermal analysis was broken at points corresponding to the main steps of decomposition and the residues in the crucible were quickly cooled in the stream of argon. This enabled to analyze the residues at strictly pre-determined steps of decomposition. The analysis was carried out using the FTIR spectroscopic techniques as well as the X-ray powder diffractometry.

The presence of crystalline phases was checked by X-ray diffraction with the use of Philips X'Pert diffractometer system. The XRPD patterns were recorded at room temperature with Cu Kα radiation (λ = 1.540 Å). Qualitative analysis of the diffraction spectra was carried out with the ICDD PDF database [29].

## 3. Results and discussion

Results of the thermal analysis of the complexes are compiled in Tables 1–3.

The $(Bu_4N)_2[MnBr_nCl_{4-n}]$ complexes have been found to undergo phase transformation preceding melting (DTA and DSC curves). Only with $(Bu_4N)_2[MnCl_4]$ the phase transformation occurs almost simultaneously with the melting as shown by overlapping peaks in the DSC curve. This precludes determination of the enthalpies of both transformations. Endothermic phase transformations occurring on heating of the complexes reveal existence of various polymorphic forms. At the phase transition temperature, bulky counter-ions execute exochoric motions. A change in the temperature of the environment results most probably in the change of the orientation of the hydrocarbon chains of the tetrabutylammonium cation in the crystal lattice of a compound, which, in turn, effectively change the environment of the $[MnBr_nCl_{4-n}]^{2-}$ ions [10,24,25]. It is also worth noting that all those transformations are irreversible. Upon cooling of a sample, corresponding peaks in the DSC curves are missing. In addition, upon repeated heating, peaks due to the transformations are missing as well. It is also interesting to note that around 280 and 230 K small endothermic transformations emerge amounting to *ca.* 2 kJ/mol which might be due to conversion of the initial metastable phase to a stable one.

**Table 1**
Temperature and enthalpy changes for physical transformations of the manganese(II) complexes as taken from the DCS curve.

| Complexes | $T_\sigma$ [K] | $\Delta H_\sigma$ [kJ/mol] | $T_m$ [K] | $\Delta H_m$ [kJ/mol] |
|---|---|---|---|---|
| $(Bu_4N)_2[MnCl_4]$ | 326 | – | 338 | 17.8[a] |
| $(Bu_4N)_2[MnBrCl_3]$ | 351 | 28.0 | 379 | 3.4 |
| $(Bu_4N)_2[MnBr_2Cl_2]$ | 352 | 26.3 | 364 | 7.6 |
| $(Bu_4N)_2[MnBr_3Cl]$ | 351 | 7.8 | 370 | 19.8 |
| $(Bu_4N)_2[MnBr_4]$ | 324 | 4.8 | 379 | 17.4 |

$T_\sigma$, Temperature of phase transformation; $\Delta H_\sigma$, enthalpy of phase transformation; $T_m$, melting point of the compound; $\Delta H_m$, enthalpy of melting.
[a] $\Delta H = \Delta H_\sigma + \Delta H_m$.

**Table 2**
Results of analysis of the decomposition products obtained in the inert atmosphere.

| Complex | Step | Temperature range [K] | $DTG_{max}$ [K] | Mass loss [%] |
|---|---|---|---|---|
| $(Bu_4N)_2[MnCl_4]$ | 1 | 440–553 | 523 | 51 |
| | 2 | 553–620 | 583 | 26 |
| | 3 | 620–695 | 658 | 4 |
| | 4 | 695–980 | 657 | 9 |
| $(Bu_4N)_2[MnBrCl_3]$ | 1 | 493–588 | 540 | 49 |
| | 2 | 588–638 | 606 | 25 |
| | 3 | 638–698 | 675 | 5 |
| | 4 | 780–998 | 949 | 17 |
| $(Bu_4N)_2[MnBr_2Cl_2]$ | 1 | 488–598 | 543 | 48 |
| | 2 | 598–678 | 598 | 27 |
| | 3 | 803–1028 | 990 | 21 |
| $(Bu_4N)_2[MnBr_3Cl]$ | 1 | 498–600 | 540 | 49 |
| | 2 | 600–648 | 624 | 25 |
| | 3 | 781–990 | 970 | 22 |
| $(Bu_4N)_2[MnBr_4]$ | 1 | 480–583 | 536 | 40 |
| | 2 | 583–650 | 607 | 25 |
| | 3 | 650–955 | 909 | 23 |

**Table 3**
Results of the analysis of the decomposition products obtained in air.

| Complex | Step | Temperature range [K] | $DTG_{max}$ [K] | Mass loss [%] |
|---|---|---|---|---|
| $(Bu_4N)_2[MnCl_4]$ | 1 | 453–573 | 518 | 53 |
| | 2 | 573–673 | 613 | 27 |
| | 3 | 673–873 | 853 | 13 |
| $(Bu_4N)_2[MnBrCl_3]$ | 1 | 473–583 | 523 | 54 |
| | 2 | 583–673 | 653 | 21 |
| | 3 | 673–883 | 873 | 13 |
| $(Bu_4N)_2[MnBr_2Cl_2]$ | 1 | 473–578 | 523 | 43 |
| | 2 | 578–673 | 653 | 30 |
| | 3 | 673–863 | 833 | 18 |
| $(Bu_4N)_2[MnBr_3Cl]$ | 1 | 453–593 | 533 | 45 |
| | 2 | 593–683 | 653 | 29 |
| | 3 | 683–893 | 863 | 18 |
| $(Bu_4N)_2[MnBr_4]$ | 1 | 473–573 | 533 | 37 |
| | 2 | 573–673 | 653 | 31 |
| | 3 | 673–873 | 853 | 17 |

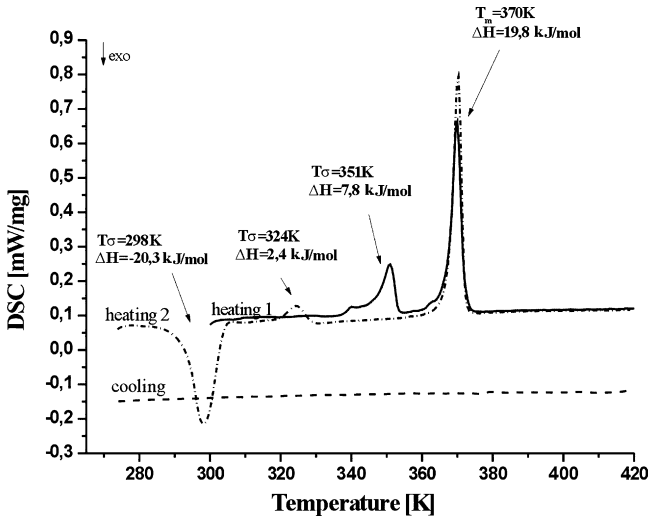


**Fig. 1.** DSC of the $(Bu_4N)_2[MnBr_3Cl]$ complex.

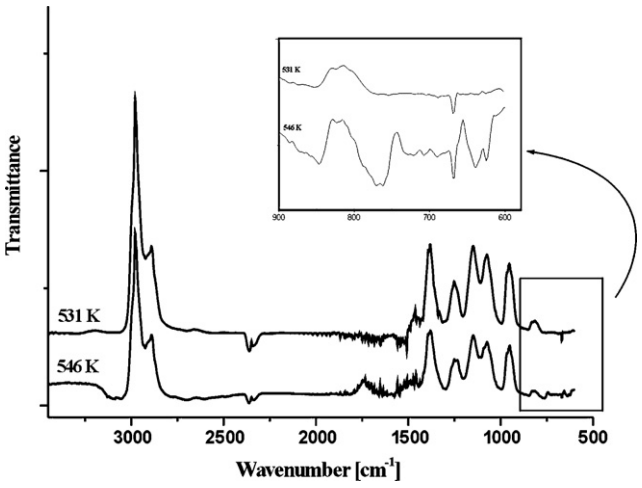


**Fig. 3.** FTIR spectra of the volatile products of the decomposition of $(Bu_4N)_2[MnCl_4]$ at 531 K and $(Bu_4N)_2[MnBr_4]$ at 546 K, in argon.

An exception is provided by $(Bu_4N)_2[MnBr_3Cl]$ (Fig. 1) where upon repeated heating a new peak emerges due to exothermic transformation ($H = -20.3$ kJ/mol).

Bis(tetrabutylammonium) tetrahalogenomanganates(II) are relatively stable in the molten state. Their thermal decomposition occurs at a temperature by more than 100 K higher than their melting points.

It should also be noticed that the pathway of the thermal transformations of the tetrahalogenomanganates(II) is affected by the kind of the halide ligand in the coordination sphere of Mn(II). For instance, upon heating of $(Bu_4N)_2[MnCl_4]$ and $(Bu_4N)_2[MnBrCl_3]$ there appear four thermal decomposition steps, whereas with the remaining complexes only three steps have been recorded. Thermal curves of exemplary compounds exhibiting either four or three endothermic steps are shown in Fig. 2.

In the FTIR spectra of the volatile decomposition products (Fig. 3), bands due to stretching C–H vibrations of the methylene and methyl groups (around 3000 cm$^{-1}$) as well as the C–N one (1450 cm$^{-1}$) could be identified. Bands below 690 cm$^{-1}$ assignable to the C–X (X = Br, Cl) bond are missing in the undecomposed compound this indicating unambiguously degradation of the cation over the temperature range of recording the spectra (*ca.* 450–650 K). A comparison of the FTIR spectra of $(Bu_4N)_2[MnCl_4]$ and $(Bu_4N)_2[MnBr_4]$ reveals both similarities (in the 3000–1400 cm$^{-1}$ range) and differences (below 1400 cm$^{-1}$) in the composition of the volatiles. As these are mixtures of compounds, their identification based on the IR spectra only turned out to be difficult. Helpful in this matter proved ionic current profiles. In the case of the bromochloromanganates(II), the ionic currents enable also to establish the sequence of volatilization of particular butyl halides. Thus, during the decomposition of $(Bu_4N)_2[MnCl_4]$ and $(Bu_4N)_2[MnBrCl_3]$ (Fig. 4) one of the first volatiles released is BuCl. Peaks at $m/z = 27$ and 41 are due to the $C_2H_3^+$ and $C_3H_5^+$ ions derived from fragmentation of the molecular ion, $C_4H_8^+$ ($m/z = 56$). Respective curves have identical shapes as a function of temperature and the intensity of particular ionic currents correspond to a BuCl spectrum filed in a spectrum library [30]. With the remaining compounds, BuBr is volatilized. Moreover, during the decomposition of all the bromochloromanganates(II) studied, $Bu_3N$ was detected among the gaseous products. A similar pattern of the decomposition of $(Bu_4N)^+$ has previously been reported [26,31–33].

Taking into account both the MS and FTIR spectra, the following equations describing thermal decomposition of the compounds in

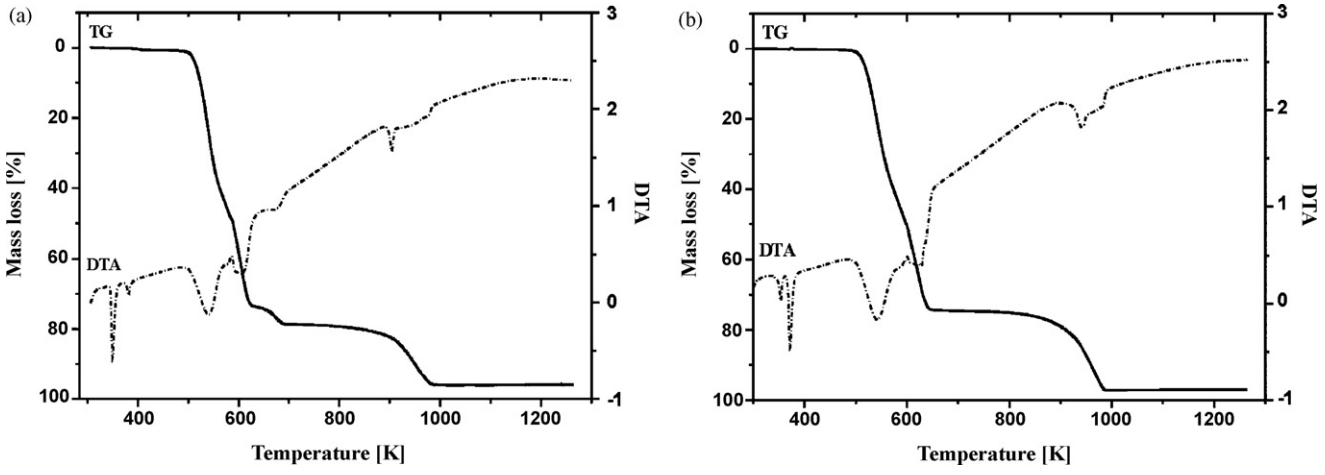


**Fig. 2.** TG and DTA traces of $(Bu_4N)_2[MnBrCl_3]$ (a) and $(Bu_4N)_2[MnBr_3Cl]$ (b) in argon.

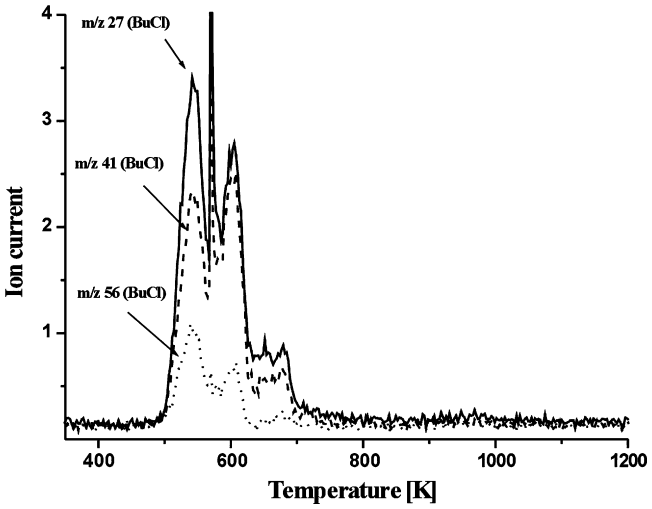


**Fig. 4.** Ionic current profiles recorded during TG–MS analysis of $(Bu_4N)_2[MnBrCl_3]$ in the inert atmosphere.

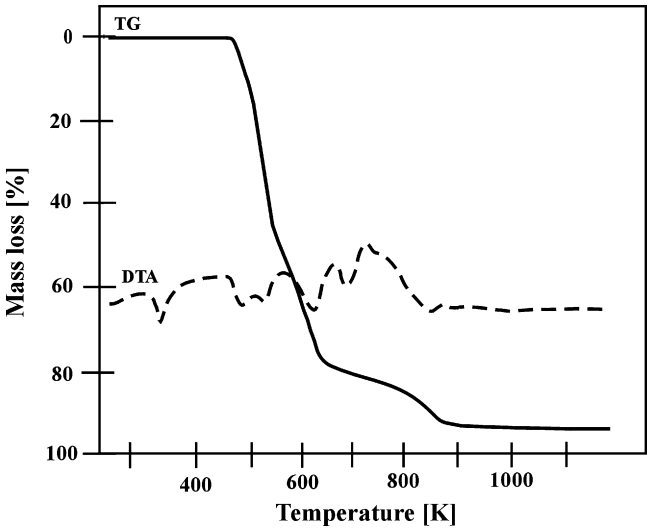


**Fig. 5.** TG and DTA curves of $(Bu_4N)_2[MnCl_4]$ in the air atmosphere.

the inert gas atmosphere can be suggested:

$$(Bu_4N)_2[MnCl_4] \xrightarrow[-Bu_3N,BuCl]{440-553\,K} (Bu_4N)[MnCl_3]$$

$$\xrightarrow[-Bu_3N,BuCl]{553-620\,K,620-695\,K} MnCl_2 + C_xH_yN_z \xrightarrow{695-980\,K} Mn, C \quad (1)$$

$$(Bu_4N)_2[MnBrCl_3] \xrightarrow[-Bu_3N,BuBr]{495-585\,K} (Bu_4N)[MnCl_3]$$

$$\xrightarrow[-Bu_3N,BuCl]{585-638\,K,638-698\,K} MnCl_2 + C_xH_yN_z \xrightarrow{790-995\,K} Mn, C \quad (2)$$

$$(Bu_4N)_2[MnBr_2Cl_2] \xrightarrow[-Bu_3N,BuCl]{488-595\,K} (Bu_4N)[MnBr_2Cl]$$

$$\xrightarrow[-Bu_3N,BuCl]{595-645\,K} MnBr_2 + C_xH_yN_z \xrightarrow{802-1027\,K} Mn, C \quad (3)$$

$$(Bu_4N)_2[MnBr_3Cl] \xrightarrow[-Bu_3N,BuBr]{495-600\,K} (Bu_4N)[MnBr_2Cl]$$

$$\xrightarrow[-Bu_3N,BuCl]{600-650\,K} MnBr_2 + C_xH_yN_z \xrightarrow{781-990\,K} Mn, C \quad (4)$$

$$(Bu_4N)_2[MnBr_4] \xrightarrow[-Bu_3N,BuBr]{478-583\,K} (Bu_4N)[MnBr_3]$$

$$\xrightarrow[-Bu_3N,BuBr]{583-650\,K} MnBr_2 + C_xH_yN_z \xrightarrow{650-955\,K} Mn, C \quad (5)$$

where $C_xH_yN_z$ is the undecomposed organic entity, Mn and C are elemental manganese and its carbide, respectively.

With $(Bu_4N)_2[MnCl_4]$ and $(Bu_4N)_2[MnBrCl_3]$ interesting are additional steps over the range 620–695 and 638–698 K, respectively, revealing formation of a stable solid phase. This is, most probably, a $Bu_3N$:$MnCl_2$ adduct resulting from interaction of the volatile tributylamine with solid $MnCl_2$. Upon further heating the adduct is decomposed leaving behind stable manganese(II) chloride. With the remaining $(Bu_4N)_2[MnBr_nCl_{4-n}]$, with $n = 2$–4, formation of a similar adduct is less probable owing to the steric hindrance. For this reason, additional decomposition steps of these compounds are missing. At the second step, $MnBr_2$ appears as the solid product. Accordingly, supplemented equations for the decomposition of the first two compounds can be written as follows:

$$(Bu_4N)_2[MnCl_4] \xrightarrow[-Bu_3N,BuCl]{440-553\,K} (Bu_4N)[MnCl_3]$$

$$\xrightarrow[-1/2Bu_3N,BuCl]{553-620\,K} \tfrac{1}{2}Bu_3N : MnCl_2 + \tfrac{1}{2}MnCl_2 + C_xH_yN_z$$

$$\xrightarrow[-1/2Bu_3N]{620-695\,K} MnCl_2 + C_xH_yN_z \xrightarrow{695-980\,K} Mn, C \quad (6)$$

$$(Bu_4N)_2[MnBrCl_3] \xrightarrow[-Bu_3N,BuBr]{495-585\,K} (Bu_4N)[MnCl_3]$$

$$\xrightarrow[-1/2Bu_3N,BuCl]{585-638\,K} \tfrac{1}{2}Bu_3N : MnCl_2 + \tfrac{1}{2}MnCl_2 + C_xH_yN_z$$

$$\xrightarrow[-1/2Bu_3N]{638-698\,K} MnCl_2 + C_xH_yN_z \xrightarrow{790-995\,K} Mn, C \quad (7)$$

An additional proof for the presence of $MnCl_2$ is a peak at 910 K in the DTA trace indicating its melting ($T_{m_{MnCl_2}} = 923$ K).

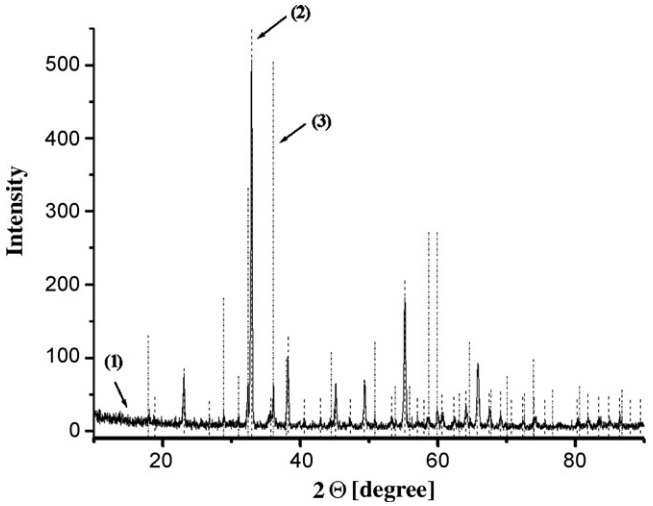


**Fig. 6.** XRPD pattern of $(Bu_4N)_2[MnCl_4]$ heated up to 900 K (1). For comparison, reflections due to $Mn_2O_3$ (2) and $Mn_3O_4$ (3) are shown.

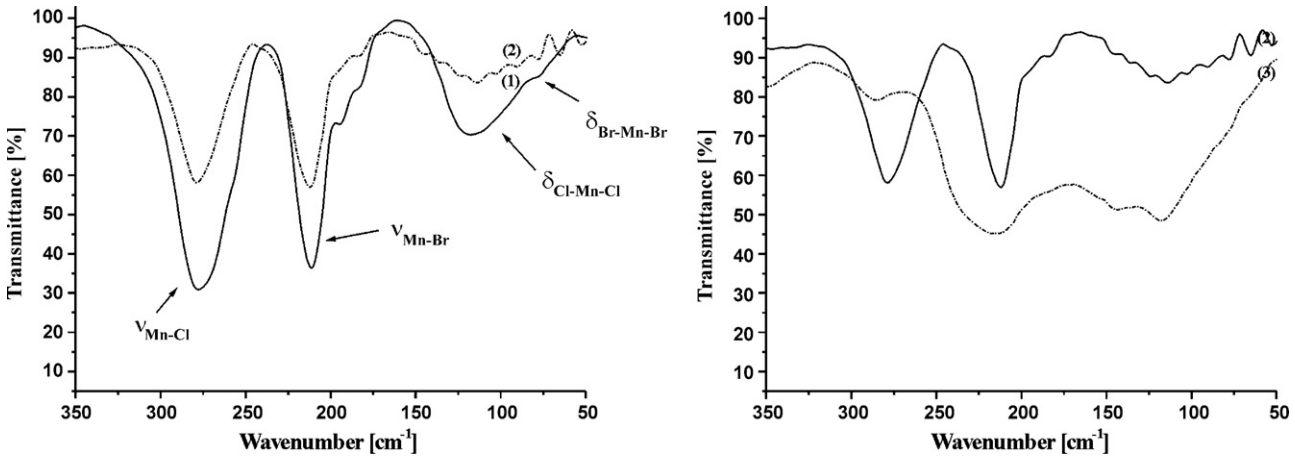


**Fig. 7.** The FT-FIR spectra of $(Bu_4N)_2[MnBr_2Cl_2]$ (1) and its decomposition products at various temperatures: $T = 573$ K (2) and $T = 653$ K (3) in argon.

Thermal decomposition of the complexes up to 650 K is endothermic and independent of the oven temperature. A solid residue left at this step is manganese(II) halide. Above 650 K the decomposition is affected by oxygen present as indicated by a variety of energetic effects seen in the DTA curves recorded in argon (Fig. 2) and in the air (Fig. 5).

A peak in the DTA curve (Fig. 5) is indicative of an exothermic course of the last step. This can be interpreted as being due to oxidation of the manganese(II) halide to manganese oxides, $Mn_2O_3$ and $Mn_3O_4$ as evidenced in the XRPD spectra of the sinters (Fig. 6).

A closer examination of the FT-FIR spectra of the sinters sampled at particular temperatures reveals differences among successive decomposition products (Fig. 7).

Thus, in the solid product of the first decomposition step of $(Bu_4N)_2[MnBr_2Cl_2]$ there are still bands due to stretching vibrations of the Mn–Cl and Mn–Br bonds at 280 and 210 $cm^{-1}$, respectively, which are missing in the products of the next step. However, on the basis of solely the Far-IR bands it was difficult to identify the final product. More helpful proved to be the X-ray powder patterns of the sinters which confirmed the presence of $MnBr_2$ in the sinters of the second step of decomposition of $(Bu_4N)_2[MnBr_2Cl_2]$ as well as the elemental manganese (in argon) and its oxides (in the air) in the final products of decomposition of $(Bu_4N)_2[MnBr_nCl_{4-n}]$ complexes (Fig. 6).

It is worth noting that inspection of the XRPD patterns revealed also $MnCl_2$ in a sinter of $(Bu_4N)_2[MnBr_2Cl_2]$ sampled at 923 K (together with a peak due to its melting). These findings suggest the decomposition of $(Bu_4N)_2[MnBr_2Cl_2]$ (Eq. (3)) to occur to a minor extent according the following reaction pathway:

$$(Bu_4N)_2[MnBr_2Cl_2] \xrightarrow[-Bu_3N,BuBr]{} (Bu_4N)[MnBrCl_2] \xrightarrow[-Bu_3N,BuBr]{} MnCl_2 \quad (8)$$

An additional proof in favour of the suggested pathway of decomposition of the manganese(II) complexes is a comparison of the percentile experimental and calculated mass losses (Table 4).

Owing to the rapid progress of the first two decomposition steps, it was difficult to determine final temperature of the first step and that of the onset of the other. In this situation the readings of the mass losses during the two steps might be burdened with a small error. Just for this reason the mass losses taken from the TG curves of the first step might be slightly larger than those calculated. It is, however, much more easily to spot a point in the

**Table 4**
Percentile experimental and calculated mass losses.

| Complex | Step | Argon | | | | Air | | | |
|---|---|---|---|---|---|---|---|---|---|
| | | Mass loss [%] | | Total mass loss [%] | | Mass loss [%] | | Total mass loss [%] | |
| | | Found | Calcd | Found | Calcd | Found | Calcd | Found | Calcd |
| $(Bu_4N)_2[MnCl_4]$ | 1 | 51 | 41 | – | – | 53 | 41 | – | – |
| | 2 | 26 | 28 | 77 | 69 | | | | |
| | 3 | 4 | 13 | 81 | 82 | 27 | 41 | 80 | 82 |
| | 4 | 9 | 10 | 90 | 92 | 13 | 7 | 93 | 89 |
| $(Bu_4N)_2[MnBrCl_3]$ | 1 | 49 | 45 | – | – | 54 | 45 | – | – |
| | 2 | 25 | 25 | 74 | 70 | | | | |
| | 3 | 5 | 13 | 79 | 83 | 21 | 38 | 75 | 83 |
| | 4 | 17 | 10 | 96 | 93 | 13 | 7 | 88 | 90 |
| $(Bu_4N)_2[MnBr_2Cl_2]$ | 1 | 48 | 36 | – | – | 43 | 36 | – | – |
| | 2 | 27 | 36 | 75 | 72 | 30 | 36 | 73 | 72 |
| | 3 | 21 | 21 | 96 | 93 | 18 | 18 | 91 | 90 |
| $(Bu_4N)_2[MnBr_3Cl]$ | 1 | 49 | 40 | – | – | 45 | 40 | – | |
| | 2 | 25 | 34 | 74 | 74 | 29 | 34 | 74 | 74 |
| | 3 | 22 | 19 | 93 | 96 | 18 | 17 | 92 | 91 |
| $(Bu_4N)_2[MnBr_4]$ | 1 | 40 | 38 | – | – | 37 | 38 | – | – |
| | 2 | 25 | 38 | 65 | 76 | 31 | 38 | 68 | 76 |
| | 3 | 23 | 18 | 88 | 94 | 17 | 15 | 85 | 91 |

TG curve corresponding to the formation of the manganese(II) halide (i.e. the end of either the second or third step). At that temperature total mass losses are comparable, thus indicating the validity of the suggested transformations. Small differences can be due to incomplete degradation of the organic matter ($C_xH_yN_z$) that becomes completely combusted only during the next step as evidenced by larger calculated and found mass losses corresponding to the final step. Similar total mass losses of the whole complex are also indicative of the presence of the suggested solid residues. In this case, small differences arise from unidentified particular components of the mixture, i.e. manganese carbide and elemental manganese in argon and $Mn_2O_3$ and $Mn_3O_4$ in air. This makes difficult a precise calculation of the total mass loss.

## 4. Conclusions

Bis(tetrabutylammonium) tetrahalogenomanganates(II) undergo irreversible endothermic phase transformations preceded by melting. The transformation temperature depends on the kind of anion. For instance, $(Bu_4N)_2[MnCl_4]$ and $(Bu_4N)_2[MnBr_4]$ undergo phase transformation at lower temperatures than the mixed-ligand halogen complexes. In the molten state, the compounds are thermally stable over the range of *ca.* 100 K and then they undergo decomposition in either three or four steps depending on the kind of anion. The volatile products of the decomposition are a butyl halide and tributylamine. The thermal decomposition of the $(Bu_4N)_2[MnCl_4]$ and $(Bu_4N)_2[MnBrCl_3]$ complexes affords a stable $Bu_3N{:}MnCl_2$ adduct at the second step. The remaining compounds are decomposed at that step to manganese(II) halide.

The course of the next step, as well as the final product, are affected by oven atmosphere. Thus, in the inert atmosphere, elemental manganese and its carbide are the final products, whereas in the oxidative atmosphere a mixture consisting of $Mn_2O_3$ and $Mn_3O_4$ is left behind. At this point, it is worth mentioning a different behaviour of $(Bu_4N)_2[MnBr_nCl_{4-n}]$ compounds and those of $(Et_4N)_2[CuBr_nCl_{4-n}]$ ones. Thus, the final product of the latter is elemental copper [28], whereas one of the final products of the manganese(II) complexes, as well as of the cobalt(II) ones [27], are the corresponding metal carbides. It can thus be concluded that the kind of the metal in the complex anion has an influence upon the pathway of thermal degradation of the $R_2[MBr_nCl_{4-n}]$ compounds, where R is an alkylammonium cation and M is a metal(II).

## Acknowledgement

This research was supported by the Polish State Committee for Scientific Research under grants DS/8232-4-0088-8 and BW/8000-5-0454-8.

## References

[1] M.L. Schultz, J. Am. Chem. Soc. 71 (1949) 1288–1292.
[2] N.S. Gill, R.S. Nyholm, J. Chem. Soc. (1959) 3997–4007.
[3] N.S. Gill, J. Chem. Soc. (1961) 3512–3515.
[4] F.A. Cotton, D.M.L. Goodgame, M. Goodgame, J. Am. Chem. Soc. 84 (1962) 167–172.
[5] J.H. Clark, T.M. Dunn, J. Chem. Soc. (1963) 1198–1201.
[6] J.R. Wiesner, R.C. Srivastava, C.H.L. Kennard, M. DiVaira, E.C. Lingafelter, Acta Crystallogr. 23 (1967) 565–574.
[7] D.R. Bloomquist, R.D. Willett, H.W. Dodgen, J. Am. Chem. Soc. 103 (1981) 2610–2615.
[8] M. Koman, V. Siroklin, G. Ondrejovič, A.B. Corradi, L.P. Battagila, Acta Crystallogr. C44 (1988) 813–815.
[9] K. Halvorson, R.D. Willett, Acta Crystallogr. C44 (1988) 2071–2076.
[10] H. Mashiyama, N. Koshiji, Acta Crystallogr. B45 (1989) 467–473.
[11] K. Hasebe, T. Asahi, Acta Crystallogr. C45 (1989) 841–843.
[12] G. Madariaga, F.J. Zúrũga, W.A. Paciorek, Acta Crystallogr. B46 (1990) 620–628.
[13] I.D. Williams, P.W. Brown, Acta Crystallogr. C48 (1992) 259–263.
[14] T. Kawata, T. Aoyama, S. Ohba, Acta Crystallogr. C49 (1993) 137–139.
[15] I.G. Gusakovskaya, S.I. Pirumowa, N.S. Ovanesyan, N.I. Golovina, R.F. Trofimova, G.V. Shilov, E.A. Lavrent'eva, Zh. Obshch. Khim. 68 (1998) 1264–1269.
[16] W. Clegg, N.C. Martin, Acta Crystallogr. E63 (2007) m1151.
[17] N.K. Iha, A. Saxena, Inorg. Chim. Acta 26 (1978) 201–205.
[18] D.M. Adams, J. Chatt, J.M. Davidson, J. Gerratt, J. Chem. Soc. (1963) 2189–2194.
[19] F.A. Cotton, R.H. Holm, J. Am. Chem. Soc. 82 (1960) 2983–2986.
[20] R. Fletcher, J.J. Hansen, J. Livermore, R.D. Willett, Inorg. Chem. 22 (1983) 330–334.
[21] Y. Fujii, Z. Wang, R.D. Willett, W. Zhang, C.P. Landee, Inorg. Chem. 34 (1995) 2870–2874.
[22] R.A. Friedman, E.G. Malawer, Y. Wei Wong, B.R. Sundheim, J. Am. Chem. Soc. 102 (1980) 925–931.
[23] M.I. Pollack, B.R. Sundheim, J. Phys. Chem. 78 (1974) 1957–1959.
[24] N. Presser, M.A. Ratner, B.R. Sundheim, Chem. Phys. Lett. 45 (1977) 572.
[25] N. Presser, M.A. Ratner, B.R. Sundheim, Chem. Phys. 31 (1978) 281.
[26] A. Bujewski, K. Grzedzicki, J. Błażejowski, Z. Warnke, J. Therm. Anal. Cal. 33 (1988) 961.
[27] E. Styczeń, Z. Warnke, D. Wyrzykowski, Thermochim. Acta 454 (2007) 84–89.
[28] E. Styczeń, W.K. Jóźwiak, M. Gazda, D. Wyrzykowski, Z. Warnke, J. Therm. Anal. Cal. 91 (2008) 979–984.
[29] ICDD PDF-2 Database Release 1998, ISNN 1084-3116.
[30] NIST Mass Spectrometry Data Center Collection (C) 2007, Number 228826.
[31] B.R. Sundheim, E. Levy, B. Howard, J. Chem. Phys. 57 (1972) 4492–4496.
[32] D. Wyrzykowski, T. Maniecki, A. Pattek-Janczyk, J. Stanek, Z. Warnke, Thermochim. Acta 435 (2005) 92–98.
[33] D. Wyrzykowski, T. Maniecki, M. Gazda, E. Styczeń, Z. Warnke, J. Therm. Anal. Cal. 90 (2007) 893–897.